

Perturbation Theory Based on a Nodal Model

Temitope A. Taiwo & A. F. Henry

To cite this article: Temitope A. Taiwo & A. F. Henry (1986) Perturbation Theory Based on a Nodal Model, Nuclear Science and Engineering, 92:1, 34-41, DOI: [10.13182/NSE86-A17862](https://doi.org/10.13182/NSE86-A17862)

To link to this article: <https://doi.org/10.13182/NSE86-A17862>



Published online: 12 May 2017.



Submit your article to this journal [↗](#)



Article views: 16



View related articles [↗](#)

Perturbation Theory Based on a Nodal Model

Temitope A. Taiwo and A. F. Henry

Massachusetts Institute of Technology, Cambridge, Massachusetts 02139

Accepted August 19, 1985

Abstract—The standard point kinetics equations and formally exact expressions for reactivity, prompt neutron lifetime, and effective delayed neutron fractions are derived from the matrix form of the nodal code QUANDRY. Perturbation theory expressions for reactivity based both on the standard quadratic-transverse-leakage form of QUANDRY and on the coarse-mesh finite difference (CMFD) form, made accurate by the use of discontinuity factors, are derived. With three-dimensional CMFD QUANDRY transient calculations taken as numerical standards, the accuracy of several standard point kinetics methods as well as the improved quasi-static method is tested. Results suggest that point kinetics methods are poor for rod ejection calculations, even if a precalculated table of rod worth versus position is used to infer the reactivity contribution of the moving rods. For transients not involving rod motion, the point kinetics equations are more accurate. Use of core-averaged (rather than node-dependent) temperature coefficients, however, can produce significant errors. The quasi-static scheme appears to yield acceptably accurate results but, for the tests run, consistently required more computing time than needed for the full three-dimensional solutions.

I. INTRODUCTION

Point kinetics¹ and quasi-static² models for describing neutron behavior in a reactor during transients account for changes in reactor conditions by determining the effect these changes have on the overall reactivity of the core. This overall reactivity is found by summing contributions from local changes in temperatures, densities, and control rod positions.

It is well known that such local contributions of reactivity are rigorously additive only if the overall shape of the flux throughout the reactor remains unaltered by the local perturbations. In practice, of course, this never happens. Thus it becomes important, in computing reactivity contributions due to local effects, to use a perturbation formula that reduces the error resulting from the neglect of local flux shape changes.

It is standard to obtain such a perturbation formula by employing adjoint flux shapes as weight functions. The usual perturbation formula that results, however, involves dot products of gradients of regular and adjoint fluxes, and finding such gradients leads either to great expense (if fine-mesh finite difference equations are used) or to great error (if only coarse-mesh nodal fluxes are available). One way around this

dilemma is to avoid the perturbation formula by performing a large number of criticality calculations (usually using a nodal model) to determine the changes in k_{eff} induced by local perturbations. This scheme, however, can also be quite expensive.

A straightforward solution to all these difficulties is to derive a perturbation theory expression for reactivity starting from the *matrix* equations that specify the nodal model rather than from the *differential* equations from which the nodal model has been derived.³ In the present paper, we develop such a perturbation theory expression for the model embodied in the nodal code QUANDRY (Refs. 4 and 5). We then test the accuracy of the point kinetics and quasi-static methods for several two- and three-dimensional test cases by comparing with corresponding QUANDRY full space-time reference calculations.

II. THEORY

QUANDRY is a three-dimensional, two-group, Cartesian geometry nodal code intended for the analysis of light water reactors. Unknowns are the node-averaged, group fluxes, and net leakages in the three coordinate directions. These are found by solving a

“nodal balance equation,” expressing the fact that the total net leakage rate out of a given node is the difference between the net rate of production and net rate of destruction of neutrons in that node, and three “coupling equations,” relating the net leakage across the node faces perpendicular to a given coordinate direction to the volume-averaged flux in the node and its two nearest neighbors in that coordinate direction, and to “transverse leakages” for the node itself and its four nearest neighbors in that coordinate direction. The coupling equations are derived analytically from

that will reproduce that solution exactly when the code is run using standard finite difference equations, which would ordinarily yield absurd answers if used with 10- to 20-cm mesh spacings. We take advantage of this situation when we investigate the accuracy of the point kinetics and quasi-static models.

If the number of nodes in the X , Y , and Z directions are I , J , and K , the total number of nodes being $N \equiv I \times J \times K$, there are, with G -energy groups, $G \times N$ unknown, node-averaged fluxes $\bar{\phi}_g^{ijk}$. The time-dependent QUANDRY nodal equations then have the form

$$\begin{bmatrix} [\mathbf{M}_p] - [\mathbf{F}] & -(h_z^k [\mathbf{G}_y] + h_y^j [\mathbf{G}_z]) & -(h_z^k [\mathbf{G}_x] + h_x^i [\mathbf{G}_z]) & -(h_y^j [\mathbf{G}_x] + h_x^i [\mathbf{G}_y]) \\ [\mathbf{F}_x] & -[\mathbf{I}] & \frac{1}{h_y^j} [\mathbf{G}_x] & \frac{1}{h_z^k} [\mathbf{G}_x] \\ [\mathbf{F}_y] & \frac{1}{h_x^i} [\mathbf{G}_y] & -[\mathbf{I}] & \frac{1}{h_z^k} [\mathbf{G}_y] \\ [\mathbf{F}_z] & \frac{1}{h_x^i} [\mathbf{G}_z] & \frac{1}{h_y^j} [\mathbf{G}_z] & -[\mathbf{I}] \end{bmatrix} \begin{bmatrix} [\bar{\phi}] \\ [\bar{L}_x] \\ [\bar{L}_y] \\ [\bar{L}_z] \end{bmatrix} + \sum_{d=1}^D \begin{bmatrix} \lambda_d [\chi_d \mathbf{C}_d] \\ [\mathbf{0}] \\ [\mathbf{0}] \\ [\mathbf{0}] \end{bmatrix} = \begin{bmatrix} [\mathbf{V}]^{-1} & [\mathbf{0}] & [\mathbf{0}] & [\mathbf{0}] \\ [\mathbf{0}] & [\mathbf{0}] & [\mathbf{0}] & [\mathbf{0}] \\ [\mathbf{0}] & [\mathbf{0}] & [\mathbf{0}] & [\mathbf{0}] \\ [\mathbf{0}] & [\mathbf{0}] & [\mathbf{0}] & [\mathbf{0}] \end{bmatrix} \frac{d}{dt} \begin{bmatrix} [\phi] \\ [\bar{L}_x] \\ [\bar{L}_y] \\ [\bar{L}_z] \end{bmatrix} \quad (1)$$

and

$$[\mathbf{M}_d][\bar{\phi}] - \lambda_d [\chi_d \mathbf{C}_d] = \frac{d}{dt} [\chi_d \mathbf{C}_d] ; \quad d = 1, 2, \dots, D, \quad (2)$$

one-dimensional, two-group diffusion equations based on homogenized group parameters for each node and with the neutron leakage rate in transverse directions approximated by a quadratic function.⁶ To correct for errors arising from the use of this quadratic transverse leakage approximation and from the use of flux-weighted values for homogenized group diffusion coefficients, the face-averaged fluxes on interior sides of all nodal surfaces are divided by “discontinuity factors.”⁷

Use of these discontinuity factors makes it possible to match reference results exactly. Moreover, discontinuity factors (along with homogenized group parameters) found from local, fine-mesh calculations (for example, zero-current boundary condition assembly or color set calculations) provide very accurate three-dimensional nodal power distributions [maximum errors $\sim 1\%$ (Ref. 8)]. It is important to note that the discontinuity factors take care of both errors in the standard procedures for finding homogenized group parameters—particularly the diffusion coefficients—and errors in the mathematical approximations used in deriving the nodal equations. Thus, if an accurate QUANDRY solution based on the analytic nodal method is available, discontinuity factors can be found

where $[\bar{\phi}]$ is the $N \times G$ column vector $\text{Col}\{\bar{\phi}_g^{ijk}\}$; the $[\bar{L}_u]$, $u = x, y, z$ are $G \times N$ column vectors of face-averaged, net nodal leakages \bar{L}_{gu}^{ijk} across node faces perpendicular to u . The vector $[\chi_d \mathbf{C}_d]$ is of length $G \times N$, its entries being the node-integrated concentrations of d 'th group precursors $V_{ijk} \bar{C}_{dijk}(t)$ ($V_{ijk} \equiv h_x^i h_y^j h_z^k$), each multiplied into the G -element column vector $\{\chi_{dg}\}$ representing the energy spectrum of neutrons emitted from group d precursors.

The matrices $[\mathbf{M}_p]$, $[\mathbf{M}_d]$, $[\mathbf{F}]$, and $[\mathbf{V}]^{-1}$ and the values of $[\mathbf{G}_u]$ and $[\mathbf{F}_u]$ are all $N \times N$ supermatrices, the elements of which are $G \times G$. [Thus they are all $(NG) \times (NG)$.] The $[\mathbf{G}_u]$ are five-stripe (each element in a stripe being $G \times G$) and account for the effect on the nodal coupling of transverse leakage perpendicular to the u direction. The values of $[\mathbf{F}_u]$ are three-stripe and relate the net leakage across the faces of a given node perpendicular to the u direction to the volume-averaged fluxes in that node and its nearest neighbors in the u direction. The elements of the

values of $[\mathbf{G}_u]$ and $[\mathbf{F}_u]$ are complicated trigonometric and hyperbolic functions of the materials buckling of the nodes.

The prompt and delayed fission neutron production matrices are block $N \times N$, the i, j, k 'th block being defined as

$$[\mathbf{M}_p^{ijk}] = V_{ijk} \sum_l (1 - \beta^l) [\chi_p^l] \frac{1}{\gamma} [\nu \Sigma_{fijk}^l(t)]^T \quad (3)$$

and

$$[\mathbf{M}_d^{ijk}] = V_{ijk} \sum_l \beta_d^l [\chi_d^l] \frac{1}{\gamma} [\nu \Sigma_{fijk}^l(t)]^T, \quad (4)$$

where

V_{ijk} = volume of the node

β_d^l = fraction of fission neutrons emitted from the d 'th precursor group for fissionable isotope $-l$ ($\beta^l \equiv \sum_{d=1}^D \beta_d^l$)

$[\chi_p^l], [\chi_d^l]$ = G -element column vectors specifying the prompt and delayed neutron spectra, respectively

γ = reactor eigenvalue k_{eff}

$[\nu \Sigma_{fijk}^l]^T$ = G -element row vector of fission neutron production cross sections for isotope l .

(A value of $k_{eff} \neq 1$ may be necessary to force the initial criticality; that value must then be retained during the transient calculation.)

Finally,

$$[\mathbf{F}] \equiv [\Sigma_T] + h_y^j h_z^k [\mathbf{F}_x] + h_x^i h_z^k [\mathbf{F}_y] + h_x^i h_y^j [\mathbf{F}_z], \quad (5)$$

where $[\Sigma_T]$ is an $N \times N$ block diagonal matrix, the ijk 'th block being $V_{ijk} [\Sigma_{Tijk}]$, the gg' element of $[\Sigma_{Tijk}]$ being $(\bar{\Sigma}_{ig}^{ijk} \delta_{gg'} - \bar{\Sigma}_{gg'}^{ijk})$.

More detailed definitions of the matrix elements and a derivation of Eqs. (1) and (2) are given in Refs. 5 and 9.

The steady-state equations corresponding to Eqs. (1) and (2) are

where $[\mathbf{M}_0] \equiv [\mathbf{M}_{p0}] + [\mathbf{M}_{d0}]$, subscript zero indicating some time-independent, reference reactor condition (usually the initial critical condition), and

$$[\mathbf{M}_{d0}] \equiv \sum_{d=1}^D [\mathbf{M}_{d0}] .$$

To obtain point kinetics equations from Eq. (1), we first introduce the "mathematical adjoint" $[\psi_0^*]$, the solution of

$$[\mathbf{H}_0]^T [\psi_0^*] = 0, \quad (7)$$

where $[\mathbf{H}_0]^T$ is the transpose of the matrix in Eq. (6). Then we define the scalar "amplitude function" $T(t)$ and a shape function $[\mathbf{S}(t)]$ by

$$\begin{aligned} T(t) &= [\psi_0^*]^T \begin{bmatrix} [\mathbf{V}]^{-1} & [\mathbf{0}] & [\mathbf{0}] & [\mathbf{0}] \\ [\mathbf{0}] & [\mathbf{0}] & [\mathbf{0}] & [\mathbf{0}] \\ [\mathbf{0}] & [\mathbf{0}] & [\mathbf{0}] & [\mathbf{0}] \\ [\mathbf{0}] & [\mathbf{0}] & [\mathbf{0}] & [\mathbf{0}] \end{bmatrix} [\psi(t)] \\ &= [\bar{\phi}_0^*]^T [\mathbf{V}]^{-1} [\bar{\phi}] \end{aligned} \quad (8)$$

and

$$\begin{aligned} [\mathbf{S}(t)] &\equiv \frac{1}{T(t)} [\psi(t)] \\ &\equiv \text{Col}\{[\mathbf{S}_\phi], [\mathbf{S}_{L_x}], [\mathbf{S}_{L_y}], [\mathbf{S}_{L_z}]\} . \end{aligned} \quad (9)$$

Finally, substituting Eq. (9) into Eq. (1), multiplying by $[\psi_0^*]^T$, and dividing the result by $[\bar{\phi}_0^*]^T [\mathbf{M}] [\mathbf{S}]$, we obtain

$$\begin{aligned} &\frac{[\bar{\phi}_0^*]^T [\mathbf{V}]^{-1} [\mathbf{S}_\phi]}{[\bar{\phi}_0^*]^T [\mathbf{M}] [\mathbf{S}_\phi]} \frac{dT(t)}{dt} \\ &= \left(\frac{[\psi_0^*]^T [\mathbf{H}] [\mathbf{S}]}{[\bar{\phi}_0^*]^T [\mathbf{M}] [\mathbf{S}_\phi]} - \frac{[\bar{\phi}_0^*]^T [\mathbf{M}_D] [\mathbf{S}_\phi]}{[\bar{\phi}_0^*]^T [\mathbf{M}] [\mathbf{S}_\phi]} \right) T(t) \\ &+ \frac{[\bar{\phi}_0^*]^T [\mathbf{V}]^{-1} [\mathbf{S}_\phi]}{[\bar{\phi}_0^*]^T [\mathbf{M}]^{-1} [\mathbf{S}_\phi]} \sum_{d=1}^D \frac{[\bar{\phi}_0^*]^T [\chi_d^l C_d]}{[\bar{\phi}_0^*]^T [\mathbf{V}]^{-1} [\mathbf{S}_\phi]}, \end{aligned} \quad (10)$$

$$\begin{bmatrix} [\mathbf{M}_0] - [\mathbf{F}_0] & -(h_z^k [\mathbf{G}_{y0}] + h_y^j [\mathbf{G}_{z0}]) & -(h_z^k [\mathbf{G}_{x0}] + h_x^i [\mathbf{G}_{z0}]) & -(h_y^j [\mathbf{G}_{x0}] + h_x^i [\mathbf{G}_{y0}]) \\ [\mathbf{F}_{x0}] & -[\mathbf{I}] & \frac{1}{h_y^j} [\mathbf{G}_{x0}] & \frac{1}{h_z^k} [\mathbf{G}_{x0}] \\ [\mathbf{F}_{y0}] & \frac{1}{h_x^i} [\mathbf{G}_{y0}] & -[\mathbf{I}] & \frac{1}{h_z^k} [\mathbf{G}_{y0}] \\ [\mathbf{F}_{z0}] & \frac{1}{h_x^i} [\mathbf{G}_{z0}] & \frac{1}{h_y^j} [\mathbf{G}_{z0}] & -[\mathbf{I}] \end{bmatrix} \begin{bmatrix} [\bar{\phi}_0] \\ [\bar{L}_{x0}^\phi] \\ [\bar{L}_{y0}^\phi] \\ [\bar{L}_{z0}^\phi] \end{bmatrix} = 0 \equiv [\mathbf{H}_0] [\psi_0], \quad (6)$$

or with the kinetics parameters defined by comparison of Eqs. (10) and (11)

$$\Lambda \frac{dT(t)}{dt} = (\rho - \beta)T(t) + \Lambda \sum_{d=1}^D \lambda_d C_d(t) \quad (11)$$

A similar manipulation of Eq. (2) yields

$$\frac{d}{dt} C_d(t) = \frac{\beta_d}{\Lambda} T(t) - \lambda_d C_d(t) \quad (12)$$

In this formal derivation of the point kinetics equations, we have used the fact [derivable from Eqs. (8) and (9)] that, although $[S(t)]$ is time dependent, $[\psi_0^*]^T [V]^{-1} [S(t)]$ is constant.

It follows from Eqs. (7), (10), and (11) that

$$\begin{aligned} \rho(t) &\equiv \frac{[\psi_0^*]^T [H_0 + \delta H] [S(t)]}{[\bar{\phi}_0^*]^T [M] [S_\phi(t)]} \\ &= \frac{[S(t)]^T [H_0]^T [\psi_0^*] + [\psi_0^*]^T [\delta H] [S(t)]}{[\bar{\phi}_0^*]^T [M] [S_\phi(t)]} \\ &= \frac{[\psi_0^*]^T [\delta H] [S(t)]}{[\bar{\phi}_0^*]^T [M] [S_\phi(t)]} \end{aligned} \quad (13)$$

Thus when $[S(t)]$ is approximated by some predetermined reference shape, the error in $\rho(t)$ is second order.

To make use of this perturbation theory expression for $\rho(t)$, it is necessary to solve Eq. (7). Unfortunately, there is at the moment no code available to do this. An alternative would be to use the QUANDRY approximation to the "physical adjoint" $[\psi_p^*]$ obtained by applying the analytical nodal method to the *differential* adjoint equations. This solution can be found by simply inputting Σ_2 , for $(1/\gamma)\nu\Sigma_{f2}$, $(1/\gamma)\nu\Sigma_{f2}$ for Σ_2 , and $\Sigma_1 + (1/\lambda)\nu\Sigma_{f1}$ for Σ_1 in the regular QUANDRY equations. However, the leakage components $[L_{up}^*]$ of $[\psi_p^*]$ will be very poor approximations to those of $[\psi_0^*]$. This can be seen by going to a limiting case of small h_u . In this limit all the terms involving any of the values of $[G_{u0}]^T$ in Eq. (7) approach zero; the other terms remain finite. Equation (7) then shows that the values of $[L_{u0}^*] \rightarrow 0$ while Eq. (6) shows that the $[L_{up}^*]$ remain finite.

In this connection it should be noted the mathematical adjoint is by no means unique. For example,

has the same solution as Eq. (6) since it can be transformed into Eq. (6) by multiplying by

$$[R] \equiv \begin{bmatrix} [I] & -h_y^j h_z^k [I] & -h_x^i h_z^k [I] & -h_x^i h_y^j [I] \\ [0] & [I] & [0] & [0] \\ [0] & [0] & [I] & [0] \\ [0] & [0] & [0] & [I] \end{bmatrix} \quad (15)$$

The mathematical adjoint of Eq. (14) (the solution of $[H_\Sigma]^T [\psi_{0\Sigma}^*] = 0$), however, differs from $[\psi_0^*]$: Since $[R][H_\Sigma] = [H_0]$, we have

$$[H_\Sigma]^T [R]^T [\psi_0^*] = [H_0]^T [\psi_0^*] = 0 \quad (16)$$

Thus

$$[\psi_{0\Sigma}^*] = [R]^T [\psi_0^*] \quad (17)$$

Lawrence³ was able to relate the physical and mathematical adjoints for a hexagonal nodal scheme by a matrix transformation. Perhaps here $[\psi_{0\Sigma}^*]$ might be approximated by the physical adjoint and $[\psi_0^*]$, then found from Eq. (17). We have not investigated this conjecture. Instead, in the present paper we make use of discontinuity factors to get around—approximately—the difficulty of solving Eq. (9) for $[\psi_0^*]$.

The approach is simple. We simply use QUANDRY in its analytical nodal form (called QUANDRY-QUAD) to find the initial, steady-state, flux leakage vector $[\psi_0]$, which is the solution of Eq. (6). Then we find discontinuity factors for each node so that the much simpler coarse-mesh finite difference (CMFD) form of QUANDRY (called QUANDRY-CMFD) also yields $[\psi_0]$. We then run reference space-time problems with QUANDRY-CMFD assuming that the initial "exact" discontinuity factors remain constant during transients. Point kinetics and quasi-static predictions of power behavior with kinetics parameters predicted using the CMFD model can then be compared with the reference space-time QUANDRY-CMFD results.

In QUANDRY-CMFD all the $[G_u]$ matrices vanish and the $[F_u]$ matrices are similar (except for the presence of discontinuity factors) to those encountered

$$[H_\Sigma][\psi_0] \equiv \begin{bmatrix} [M_0] - [\Sigma_T] & -h_y^j h_z^k [I] & -h_x^i h_z^k [I] & -h_x^i h_y^j [I] \\ [F_{x0}] & -[I] & \frac{1}{h_y^j} [G_{x0}] & \frac{1}{h_z^k} [G_{x0}] \\ [F_{y0}] & \frac{1}{h_x^i} [G_{y0}] & -[I] & \frac{1}{h_z^k} [G_{y0}] \\ [F_{z0}] & \frac{1}{h_x^i} [G_{z0}] & \frac{1}{h_y^j} [G_{z0}] & -[I] \end{bmatrix} \begin{bmatrix} [\bar{\phi}_0] \\ [\bar{L}_{x0}] \\ [\bar{L}_{y0}] \\ [\bar{L}_{z0}] \end{bmatrix} = 0 \quad (14)$$

with finite difference approximations. The expression for reactivity reduces to

$$\rho(t) = \frac{[\bar{\phi}_0^*]^T [\delta \mathbf{M} - \delta \mathbf{F}] [\mathbf{S}_\phi(t)]}{[\bar{\phi}_0^*]^T [\mathbf{M}] [\mathbf{S}_\phi(t)]}, \quad (18)$$

and Eq. (7) for $[\psi_0^*]$ yields $[\mathbf{L}_{u_0}^*] = 0$, $u = x, y, z$, and

$$[\mathbf{M}_0^T - \mathbf{F}_0^T] [\bar{\phi}_0^*] = 0, \quad (19)$$

which can be solved fairly simply by reordering some terms in QUANDRY-CMFD.

The assumption that the discontinuity factors remain constant during a transient is of course not completely valid. However, it can be tested by comparing QUANDRY-QUAD and QUANDRY-CMFD analyses of the same space-time transient. Doing so yields errors of <5% for transients during which the power doubles. Because of this we believe that the comparisons between space-time and point kinetics methods presented in Sec. III (all based on CMFD calculations using time-independent discontinuity factors) provide meaningful information.

III. NUMERICAL RESULTS

The point kinetics equations [Eqs. (11) and (12)] are formally exact in that, if $\rho(t)$ is computed by Eq. (18), the $T(t)$ that results from solving Eqs. (11) and (12) will be identical with the value obtained directly from the three-dimensional solution $[\psi(t)]$ by use of Eq. (8). In practice, of course, $[\mathbf{S}_\phi(t)]$ in Eq. (18) must be approximated. In the present paper, we test two standard approximations:

1. point kinetics, in which $[\mathbf{S}_\phi(t)]$ is replaced by $[\bar{\phi}_0]$, the initial steady-state flux shape
2. "improved quasi-static approximation,"² in which the shape is updated from time to time in accordance with the changing reactor conditions.

The updated shape is found by substituting $[\bar{\phi}] = [\mathbf{S}_\phi]T(t)$ into (the CMFD form of) Eqs. (1) and (2) and solving that equation for a fairly large time interval between, say, t_n and t_{n+1} . To do this, one needs $(1/T)(dT/dt)$ evaluated at t_n and t_{n+1} . Accordingly, the point kinetics equations are solved at a sequence of more closely spaced times, $t_n^p = 1, 2, \dots, P$ in the range $t_n \rightarrow t_{n+1}$. Reactivity values at the t_n^p are needed to carry out this procedure, and, for the first pass through the interval $(t_{n+1} - t_n)$, these are found from Eq. (8) using $[\mathbf{S}_\phi(t_n)]$ and the latest thermal-hydraulic and control rod conditions at the intervening times t_n^p . {Thermal-hydraulic conditions are calculated using the reconstructed flux $[\bar{\phi}(t_n^p)] = [\mathbf{S}_\phi(t_n)]T(t_n^p)$.} An updated shape $[\mathbf{S}_\phi^{(1)}(t_{n+1})]$ at t_{n+1} is calculated from Eqs. (1) and (2), using a single time step $(t_{n+1} - t_n)$ and, if the reactivity computed from this shape at t_{n+1}

does not agree within a small error with that computed at that time using $[\mathbf{S}_\phi(t_n)]$, the point kinetics calculations within the interval are rerun, this time approximating $[\mathbf{S}_\phi(t)]$ in expression (18) for $\rho(t)$ by the linear relationship $\langle [\mathbf{S}_\phi(t_n)](t_{n+1} - t) + [\mathbf{S}_\phi^{(1)}(t_{n+1})] \times (t - t_n) \rangle \div (t_{n+1} - t_n)$. A new updated shape $\mathbf{S}_\phi^{(2)}(t_{n+1})$ is calculated by again solving Eqs. (1) and (2) for a single time step, and the associated reactivity is compared with that computed at the end of the first pass. The process is continued to convergence, and the whole procedure is repeated for the next large time interval $(t_{n+2} - t_{n+1})$.

The quasi-static approximation automatically takes care of flux shape changes due to control rod motion. The point kinetics scheme based on the perturbation formula cannot do this, and hence is expected to lead to serious errors if applied to a transient involving rod motion. A common procedure for avoiding this difficulty is to perform a series of criticality calculations for beginning of transient thermal conditions but with the control rod (or rods) in various positions expected during the transient. A table of reactivity versus rod location under constant thermal conditions is then created and used during the transient. Thermal feedback effects are still accounted for by the perturbation formula based on flux and adjoint shapes for the control rods in some fixed, reference position. The total reactivity at any time is then the sum of these two contributions.

We have run small test problems to evaluate the accuracy of this hybrid scheme as compared with the point kinetics perturbation theory method and with the quasi-static approach. Also, we have investigated the error arising from use of reactor-averaged temperature coefficients. Both two- and three-dimensional situations have been examined.¹⁰ We describe, however, only three, three-dimensional tests, the first two involving control rod withdrawal, with and without thermal feedback, and the third simulating a cold water accident.

Figure 1 shows horizontal cross sections of the upper portions of the two- and three-dimensional reactors studied. The reactor in Fig. 1a is 60 cm high with the control rod initially present only in the upper half. The reactor in Fig. 1b is 63 cm high and has control rods only in the top 42 cm. The homogenized fuel compositions (labeled 3-7 in Fig. 1a and 1-3 in Fig. 1b) are representative of a pressurized water reactor (PWR), (2, 6, and 7) being almost identical and more highly enriched than [1, 2, and 3 (in Fig. 1a)]. For Fig. 1a, the two-group albedo matrices $[\alpha]$ simulate the presence of a core baffle followed by a water reflector, and albedos simulating a pure water reflector are used axially. For Fig. 1b, the radial boundary conditions are as indicated, and axial conditions are $\phi_g = 4\mathbf{n} \cdot \mathbf{J}_g$, the attempt being to simulate an interior region of a PWR. The two-group homogenized cross sections used are given in Ref. 10. For cases involving

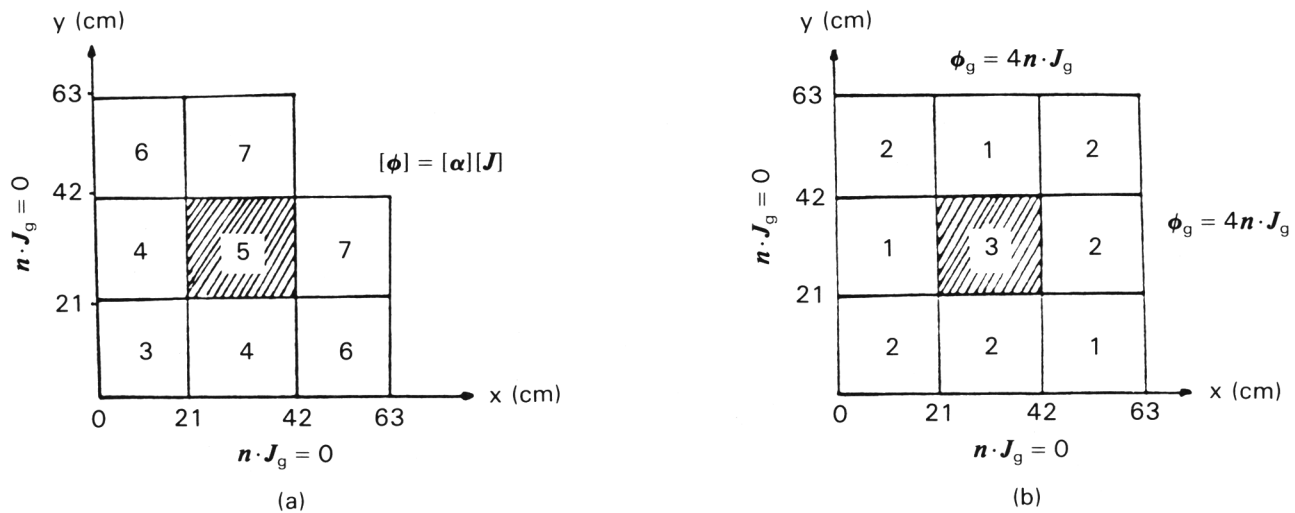


Fig. 1. Horizontal cross sections of upper portions of test reactors. The shaded area represents the rodded region.

feedback, thermal conditions are followed for each node, a simple, nonboiling, one-dimensional thermal-hydraulics model being used (the WIGL model¹¹ programmed into QUANDRY).

Table I shows the results of removing the central rod at a rate of 150 cm/s for 0.08 s with thermal feedback effects neglected. Column 2 shows dramatically that the effect on flux shape due to rod motion must be factored into the expression for reactivity if large errors are to be avoided. (Errors are shown in parentheses.) It might at first be thought that the use of rod worth tables would overcome the difficulty completely. However, column 3 shows that such is not the case. The reason is that the true flux shape $[S_o(t)]$ required for Eq. (18) to be exact is one associated with a fast exponential rise and, because of the kinetic distortion term $[(1/T)(dT/dt)]$, differs from the critical flux shape used to calibrate the rod. The quasi-static scheme provides reasonable accuracy. Its running

time, however, is ~ 4 times that of the three-dimensional standard.

Table II shows results for the same rod withdrawal, but with thermal feedback included. Point kinetics based on perturbation theory is not shown; it is again very inaccurate, yielding a predicted normalized power of 2.17 at 0.2 s, when the reference value is 10.10. What is very surprising is that, for the point kinetics model, when the rod worth contributions to reactivity are taken from the precomputed table, results are even worse. Since the kinetics distortion term produces a much smaller error even when the transient is much faster (Table I), the error here must be due to the fact that the temperature feedback contributions to reactivity were determined using the initial, unperturbed flux shape and adjoint. Whether the feedback is computed from local or core-averaged temperatures does not seem to matter nearly as much. Again the quasi-static method produces accurate

TABLE I
Control Rod Withdrawal Problem Without Feedback; Normalized Reactor Power Versus Time

Time (s)	Three-Dimensional CMFD QUANDRY Reference	Point Kinetics (Rod Worth by Perturbation Theory)	Point Kinetics (Rod Worth from Table)	Quasi-Static (6 Flux Updates)
0.000	1.000	1.000	1.000	1.000
0.050	2.386	1.702 (-28.7)	2.381 (0.2)	2.345 (1.8)
0.100	20.569	2.742 (-86.7)	19.551 (-5.0)	18.940 (-7.9)
0.150	100.817	2.828 (-97.2)	89.155 (-11)	95.800 (-5.0)
0.200	393.426	2.849 (-99.2)	321.118 (-18)	393.155 (-0.1)
Computation time	(5.5)	(2.24)	(1.86)	(23.05)

TABLE II
Control Rod Withdrawal Problem with Feedback; Normalized Reactor Power Versus Time

Time (s)	Three-Dimensional CMFD QUANDRY Reference	Point Kinetics (Rod Worth from Table; Feedback from Core-Averaged Temperature)	Point Kinetics (Rod Worth from Table; Feedback from Local Temperatures)	Quasi-Static (11 Flux Update)
0.000	1.00000	1.00000	1.00000	1.00000
0.050	2.02716	2.38341 (17.6)	2.38127 (17.5)	1.98194 (-2.2)
0.100	6.87888	19.47240 (183)	19.54880 (184)	6.67886 (-2.9)
0.200	10.09550	150.24200 (1388)	125.3680 (1141)	9.96237 (-1.3)
0.700	5.02341	2.99543 (-40)	2.71196 (-46)	5.01442 (-0.2)
1.200	3.13405	1.94288 (-38)	1.91468 (-39)	3.15282 (0.6)
Computation time	(6.67)		(2.86)	(26.36)

results, but its running time still exceeds that of the reference by a factor of ~ 4 .

For the variable inlet coolant temperature problem, we used a three-dimensional reactor model for which Fig. 1b shows a radial cross section of the upper half. The lower half is the same except that the rodded region 3 is replaced by unrodded material 1. The transient is induced by changing the temperature of the inlet coolant according to the formula $T_{cin} = 533 - 37.3333t + 20.00t^2$, where t is in seconds. The inlet flow rate (held constant) is such that the coolant passes through the axial zone being modeled in ~ 0.6 s. The control rod is kept fixed in position throughout the 1.6-s interval during which the transient is followed. Table III shows the results. The point kinetics with reactivity feedback computed as a sum of contributions from every node (column 3) does fairly well once the colder entering water has reached the outlet of the axial zone (~ 0.6 s). On the other hand, use of a core-averaged temperature coefficient yields results signifi-

cantly different from the reference values. With 18 flux updates the quasi-static method is fairly accurate. Again, however, the computation time is longer (a factor of 2). (With only 10 flux updates the computation time is reduced to 9.2 s; however, the maximum error increases to 11.3%.)

IV. CONCLUSIONS

General conclusions concerning the theory presented in this paper can be stated with more confidence than those relating to the numerical results. The procedure for obtaining the point kinetics equations and the corresponding perturbation expression for reactivity has been applied to the QUANDRY nodal model. It is applicable, however, to any nodal model for which the defining equations can be cast in a linear matrix form. As a result, node-dependent reactivity coefficients can be edited from at most two, three-dimensional nodal calculations.

TABLE III
Variable Inlet Temperature Flow Problem with Feedback; Normalized Reactor Power Versus Time

Time (s)	Three-Dimensional CMFD QUANDRY Reference	Point Kinetics (Feedback from Core-Averaged Temperature)	Point Kinetics (Feedback from Local Temperatures)	Quasi-Static (18 Flux Updates)
0.0	1.00000	1.00000	1.00000	1.00000
0.2	1.89087	1.64442 (-13.0)	1.64098 (-13.2)	1.88758 (-0.2)
0.4	5.52793	3.43494 (-37.9)	3.26028 (-41.0)	5.60374 (1.4)
0.6	11.09740	27.66200 (149.3)	11.07470 (-0.2)	10.70220 (-3.6)
0.8	7.80197	13.32640 (70.8)	7.30756 (-6.3)	7.73877 (-0.8)
1.0	5.40020	9.32945 (72.8)	5.26561 (-2.5)	5.44461 (0.8)
1.2	3.59296	6.01209 (67.3)	3.65653 (1.8)	3.72162 (3.6)
1.4	2.34338	3.83647 (63.8)	2.50223 (6.8)	2.46688 (5.3)
1.6	1.54674	2.50007 (61.6)	1.72007 (11.2)	1.63752 (5.9)
Computation time	(7.26)	(2.35)	(2.07)	(14.21)

The accuracy of the reactivity coefficients will depend on the accuracy of the underlying nodal model. We feel that coefficients derived from the QUANDRY-CMFD model should be correct to a few percent. However, we intend to continue the search for an efficient way to find the solution to the QUANDRY-QUAD adjoint equations so that the assumption of time-independent CMFD discontinuity factors will not be necessary.

The numerical test cases suggest that the point kinetic analysis is invalid for rod withdrawal transients, that one should always use node-dependent rather than average reactivity coefficients, and that the quasi-static method, while acceptably accurate, is more expensive than a full three-dimensional space-time nodal calculation. Clearly a greater number and a greater variety of test problems must be run before the present inferences should be considered firm conclusions. If, however, our tentative conclusions hold up, it may be necessary to modify certain current design procedures. Fortunately, transient nodal codes capable of providing the needed reference calculations are now becoming available.¹²

ACKNOWLEDGMENT

This study was supported by Northeast Utilities Service Company, Pacific Gas and Electric Company, PSE&G Research Corporation, and Consolidated Edison Company of New York.

REFERENCES

1. A. F. HENRY, *Nucl. Sci. Eng.*, **3**, 52 (1958).
2. D. A. MENELEY, K. O. OTT, and E. S. WEINER, "Further Developments of the Quasi-Static Neutron Kinetics Model," ANL-7410, p. 398, Argonne National Laboratory (1969).
3. R. D. LAWRENCE, "A Nodal Method for Three-Dimensional Fast Reactor Calculations in Hexagonal Geometry," *Proc. Topl. Mtg. Advances in Reactor Computations*, Salt Lake City, Utah, March 28-31, 1983, Vol. II, p. 1030, American Nuclear Society (1983).
4. G. GREENMAN, K. SMITH, and A. F. HENRY, "Recent Advances in an Analytic Nodal Method for Static and Transient Reactor Analysis," *Proc. Topl. Mtg. Computational Methods in Nuclear Engineering*, Williamsburg, Virginia, April 23-25, 1979, Vol. I, p. 3-49, U.S. Department of Energy (1979).
5. K. S. SMITH, "An Analytic Nodal Method for Solving the Two-Group, Multidimensional, Static and Transient Neutron Diffusion Equation," Nuclear Engineer's Thesis, Massachusetts Institute of Technology, Department of Nuclear Engineering (Mar. 1979).
6. H. FINNEMANN, F. BENNEWITZ, and M. R. WAGNER, "Interface Current Techniques for Multidimensional Reactor Calculations," *Atomkernenergie*, Bd. 30 (1977).
7. K. S. SMITH, A. F. HENRY, and R. A. LORETZ, "The Determination of Homogenized Diffusion Theory Parameters for Coarse Mesh Nodal Analysis," *Proc. Conf. 1980 Advances in Reactor Physics and Shielding*, Sun Valley, Idaho, September 14-17, 1980, p. 294, American Nuclear Society (1980).
8. M. H. CHANG, HAN-SEM JOO, J. PÉREZ, and A. F. HENRY, "Some Applications of Discontinuity Factors for Reactor Physics Calculations," *Proc. Topl. Mtg. Reactor Physics and Shielding*, Chicago, Illinois, September 17-19, 1984, Vol. 1, p. 185, American Nuclear Society (1984).
9. K. SMITH, "Spatial Homogenization Methods for Light Water Reactor Analysis," PhD Thesis, Massachusetts Institute of Technology, Department of Nuclear Engineering (June 1980).
10. T. A. TAIWO, "The Quasi-Static Nodal Method for Reactor Core Kinetics," PhD Thesis, Massachusetts Institute of Technology, Department of Nuclear Engineering (Oct. 1984).
11. A. V. VOTA, N. J. CURLEE, and A. F. HENRY, "WIGL-3—A Program for the Steady-State and Transient Solution of the One-Dimensional, Two-Group, Space-Time Diffusion Equations Accounting for Temperature, Xenon and Control Feedback," WAPD-TM-788, Bettis Atomic Power Laboratory (1969).
12. D. P. GRIGGS, M. S. KAZIMI, and A. F. HENRY, "TITAN: An Advanced Three Dimensional Coupled Neutronic/Thermal-Hydraulics Code for Light Water Nuclear Reactor Core Analysis," MIT-EL 84-011, Massachusetts Institute of Technology, Energy Laboratory (June 1984).